ACS APPLIED MATERIALS & INTERFACES

Research Article

www.acsami.org

Harvesting Triplet Excitons with Exciplex Thermally Activated Delayed Fluorescence Emitters toward High Performance Heterostructured Organic Light-Emitting Field Effect Transistors

Li Song,[†,‡] Yongsheng Hu,[*,†] Zheqin Liu,[†] Ying Lv,[†] Xiaoyang Guo,[†] and Xingyuan Liu[*,†]

[†]State Key Laboratory of Luminescence and Applications, Changchun Institute of Optics, Fine Mechanics and Physics, Chinese Academy of Sciences, Changchun 130033, China

[‡]University of Chinese Academy of Sciences, Beijing 100049, China

Supporting Information

ABSTRACT: The utilization of triplet excitons plays a key role in obtaining high emission efficiency for organic electroluminescent devices. However, to date, only phosphorescent materials have been implemented to harvest the triplet excitons in the organic light-emitting field effect transistors (OLEFETs). In this work, we report the first incorporation of exciplex thermally activated delayed fluorescence (TADF) emitters in heterostructured OLEFETs to harvest the triplet excitons. By developing a new kind of exciplex TADF emitter constituted by m-MTDATA (4,4′,4″-tris(*N*-3-methylphenyl-*N*-phenylamino)triphenylamine) as the donor and OXD-7 (1,3-bis[2-(4-*tert*-butylphenyl)-1,3,4-oxadiazo-5-yl]benzene) as the acceptor, an exciton utilization efficiency of 74.3% for the devices was achieved. It is found that the injection barrier between hole transport layer and emission layer as well as the ratio between donor and acceptor would influence the external quantum efficiency (EQE) significantly. Devices with a maximum EQE of 3.76% which is far exceeding the reported results for devices with conventional fluorescent emitters were successfully demonstrated. Moreover, the EQE at high brightness even outperformed the result for organic light-emitting diode based on the same emitter. Our results demonstrate that the exciplex TADF emitters can be promising candidates to develop OLEFETs with high performance.

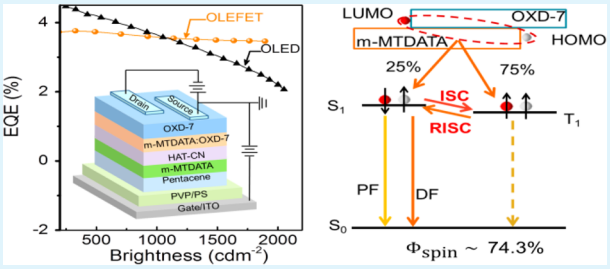

KEYWORDS: *exciplex, light-emitting, field-effect transistors, thermally activated delayed florescence, triplet excitons, reverse intersystem crossing*

INTRODUCTION

Organic light-emitting field effect transistors (OLEFETs) have emerged as a promising element in simplified displays, integrated optical communication, and even electrically driven organic lasers, mainly due to their unique characteristic of combining the switching property of a transistor and the emitting property of an organic light-emitting device (OLED).[1−6] Among the emerged device structures of single layer,[7,8] bilayer,[9] and multilayer,[10,11] the multilayer heterostructured OLEFETs (HOLEFETs) have shown superior optical and electrical characteristics in terms of brightness, external quantum efficiency (EQE), on/off ratio, as well as aperture ratio due to their flexibility of incorporating emission layer (EML) with high emission efficiency and charge transport layer (CTL) with high carrier mobilities simultaneously.[12−14] Despite the significant advances of the optical performance for the HOLEFETs, it is still much inferior to that of the OLEDs, especially that the EQE at high brightness, which is of practical significance, can hardly compete with that for OLED with an identical emission layer.[13,15−17] It is also noticed that the recent advances mainly benefited from the improvement of the charge injection and transport ability. For instance, strategies such as asymmetric source/drain electrodes,[18] interfacial modification,[19] developing new CTLs with high mobility[12] have been proposed. Whereas the exciton utilization of the EML also plays a crucial role on the device perfomance, it is far from been satisfactorily investigated.

Harvesting triplet excitons is known to be an effective route to promoting the optical performance for organic electroluminescence devices including HOLEFETs.[20−23] For instance, HOLEFETs with phosphorescent emitters have presented superior performance than those with conventional fluorescent emitters by virtue of better utilization of the triplet excitons.[13] Unfortunately, phosphorescent emitters suffer from expensive and nonrenewable heavy metals which would restrict the practical application in the future. Besides, phosphorescent emitters are often dispersed in host materials to suppress the concentration quenching,[24] whereas the hosts normally have large bandgaps that will cause large energy barriers between the CTLs and EML and subsequently result in unbalanced carrier

Received: October 20, 2016
Accepted: December 28, 2016
Published: December 28, 2016

DOI: 10.1021/acsami.6b13405
ACS Appl. Mater. Interfaces 2017, 9, 2711−2719

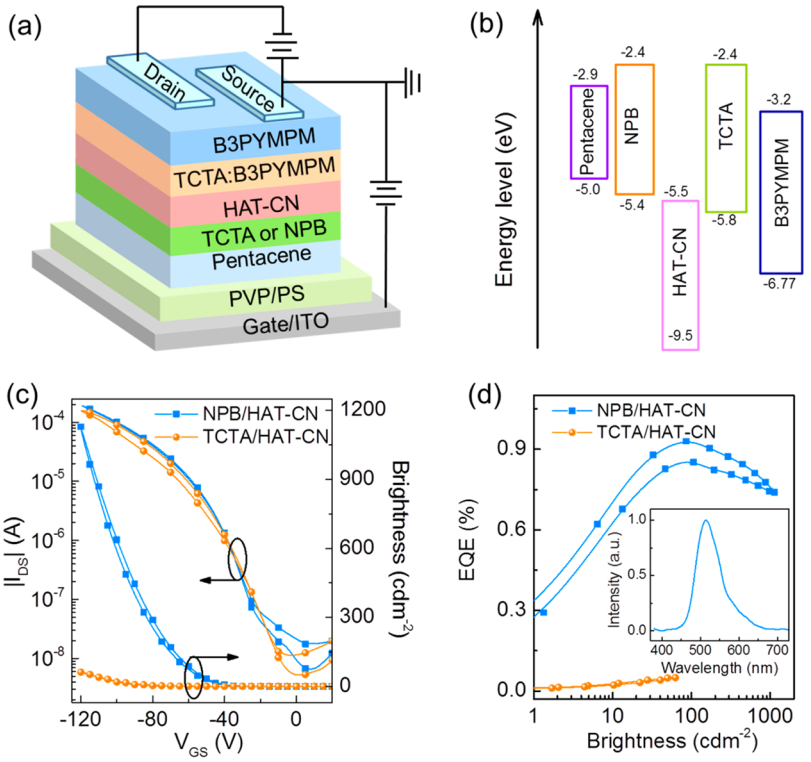

Figure 1. (a) Schematic of the device structure. (b) Energy-level diagram of the organic active materials. (c) Electrical and optical transfer characteristics for HOLEFETs with TCTA/B3PYMPM exciplex TADF emitter at V_{DS} = −80 V. (d) Corresponding relationship between EQE and brightness at V_{DS} = −80 V. Inset is the EL spectrum of the device.

injection into the EML. It is therefore necessary to explore alternatives to make use of the triplet excitons in HOLEFETs.

Thermally activated delayed fluorescence (TADF)[25,26] is a novel strategy to utilize the triplet excitons via the reverse intersystem crossing (RISC) and has already inspired a new wave of research in OLEDs owing to their potential of low cost and high performance.[27,28] An essential prerequisite for efficient up-conversion from triplet state to singlet state is a small energy gap (ΔE_{ST}) between the lowest triplet excited state (T_1) and singlet excited state (S_1), which requires small spatial overlap between the highest occupied molecular orbital (HOMO) and lowest unoccupied molecular orbital (LUMO) of the emitter.[25,29] The well-designed electron donor−acceptor TADF molecules can satisfy this requirement; however, they are usually needed to be doped in host materials whose energy bandgaps[27] would cause large energy barriers with the CTLs for common HOLEFETs. Alternatively, the exciplex emitter composed of physical mix of a donor molecule and an acceptor molecule inherently also has small ΔE_{ST} since it has delocalized HOMOs centered at the donor and LUMOs centered at the acceptor, respectively,[26,30,31] ensuring it as an important class of TADF emitters in OLEDs. Another merit of incorporating the exciplex TADF emitters in OLEDs is that low turn-on voltage[32−36] can be achieved due to the low HOMO level of the donors and the high LUMO level of the acceptors which could lower the energy barriers between the CTLs and the EML. This feature could also be attractive for overcoming the energy barriers between the CTLs with high mobility and the EML in the HOLEFETs if exciplex TADF emitters were implemented. Despite these advantages for exciplex TADF emitters, they have not yet been demonstrated as the EML in the HOLEFETs.

In this study, we reported the first incorporation of exciplex TADF emitters in HOLEFETs to harvest the triplet excitons. The feasibility of harvesting the triplet excitons was confirmed by using the exciplex of TCTA ((4,4′,4″-tris(*N*-carbazolyl)-triphenylamine):B3PYMPM (bis-4,6-(3,5-di-3-pyridylphenyl)-2-methylpyrimidine), which shows an exciton utilization efficiency of 60.3% with a maximum EQE of 0.93% for the devices. We further developed a new kind of exciplex TADF emitter constituted by m-MTDATA (4,4′,4″-tris(*N*-3-methylphenyl-*N*-phenylamino)triphenylamine) as the donor and OXD-7 (1,3-bis[2-(4-*tert*-butylphenyl)-1,3,4-oxadiazo-5-yl]-benzene) as the acceptor, which shows better aligned HOMO levels between the hole transport layer and the exciplex donor as well as improved exciton utilization efficiency of 74.3% for the devices. Consequently, a much enhanced maximum EQE of 3.76% with an on/off ratio of ~10^4 was successfully achieved for the devices. Moreover, the EQE at brightness exceeding 1100 cdm^{-2} even outperforms the result for the OLED based on the same emitter. Our study not only demonstrates that the exciplex TADF emitters can be promising candidates for developing high performance HOLEFETs but also provides some insights for the construction of exciplex based HOLEFETs.

RESULTS AND DISCUSSION

A well-known exciplex TADF emitter composed of TCTA (donor) and B3PYMPM (acceptor) was investigated first since it exhibits efficient RISC process in OLEDs and a moderate photoluminescence quantum yield (PLQY) (36%).[37] Figure 1a shows the schematic of the device structure. Pentacene acted as the hole transport layer due to its high hole mobility. In our previous work, we found that organic heterojunction (OHJ)

DOI: 10.1021/acsami.6b13405
ACS Appl. Mater. Interfaces 2017, 9, 2711−2719

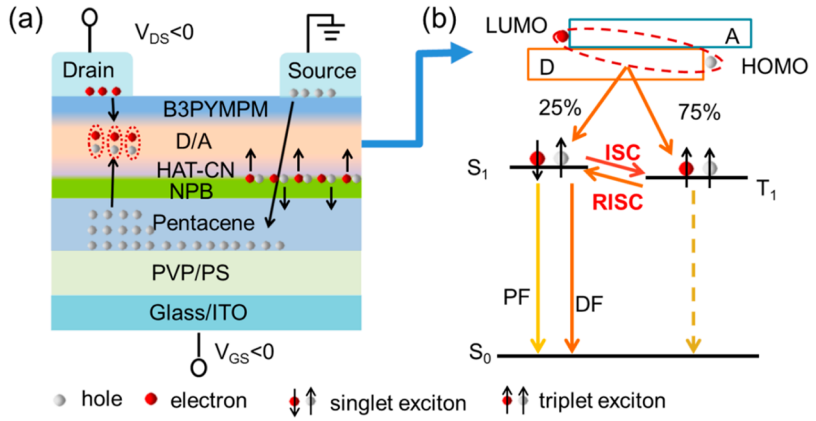

Figure 2. (a) Schematic representation of the carrier injection and transport as well as the light emission mechanism. The arrow denotes the transport direction of the carriers. (b) Process for harvesting triplet excitons in the mixed TCTA:B3PYMPM film under electrical excitation. D, A, PF, DF represent the donor, acceptor, prompt fluoresence, and delayed fluorescence.

consists of a p-type organic molecule and 1,4,5,8,9,11-hexaazatriphenylenehexacarbonitrile (HAT-CN) can be used as a modification layer to improve the carrier injection and transport for HOLEFETs.[13] Therefore, here we adopt TCTA/HAT-CN as an OHJ modification layer. The charge transfer process between TCTA and HAT-CN can be verified by the absorption spectrum where an additional absorption peak around 520 nm appears for the mixed TCTA:HAT-CN film compared with that for pure TCTA and HAT-CN films (see Figure S1). B3PYMPM was used as the electron injection layer as well as hole blocking layer. Considering the large HOMO level offset between pentacene and TCTA as shown in Figure 1b, a device with another OHJ modification layer of NPB (*N*,*N*′-di(naphthalene-1-yl)-*N*,*N*′-diphenylbenzidine)/HAT-CN was also fabricated for comparison. The molecular structures for the organic active layers are shown in Figure S2.

Figure 1c presents the transfer characteristics for devices with different OHJ modification layers at drain to source voltage V_{DS}= −80 V. Both devices exhibit quite similar electrical properties that are typical p-type characteristics. The on/off ratio is ∼10^4 within the test range. The maximum drain current (I_{DS}) is more than 2 orders of magnitude higher compared with that for devices without the OHJ modified layer (see Figure S1b), which can be mainly attributed to the extra charges generated in the OHJ modification layers. The brightness for both devices increases as the drain current becomes larger. However, the maximum brightness for NPB/HAT-CN modified device (1116 cdm^{-2}) is much higher than that for TCTA/HAT-CN modified one (62 cdm^{-2}). The maximum EQE for TCTA/HAT-CN modified device is 0.05% (Figure 1d), while that for NPB/HAT-CN modified device shows a much enhanced value of 0.93% and is well maintained above 0.75% at the brightness of 1000 cdm^{-2}. The inferior optical performance for TCTA/HAT-CN modified device can be attributed to the larger hole injection barrier between the HOMO levels of pentacene and TCTA than NPB (see Figure 1b). The replacement of TCTA by NPB could lower the barrier and thus facilitate the hole injection from pentacene to the TCTA/B3PYMPM emitter. The inset in Figure 1d gives the EL spectrum with a peak of ∼510 nm, which coincides well with the reported result.[37] Since the reported photoluminescent spectrum shows a peak around ∼490 nm,[37] there is a red-shift for the EL spectrum, which probably comes from the enhanced proportion of the delayed fluorescence under EL excitation.[26]

Although the maximum EQE of 0.93% for the HOLEFET is inferior to that of OLED with the TCTA/B3PYMPM exciplex emitter, it is comparable to the state-of-the-art results for HOLEFETs with conventional fluorescent emitters.[12,38−40] Considering the relatively low PLQY, we attribute the high EQE to the efficient utilization of triplet excitons. For a better understanding, we present the detailed operating mechanism of the devices in Figure 2. When the devices are working in the hole accumulation mode (gate to source voltage V_{GS} < 0, V_{DS} < 0), the holes will inject from the source electrode and move downward to pentacene. Meanwhile, holes can also be generated at the NPB/HAT-CN OHJ via the charge transfer process.[41] The injected holes as well as the generated holes will accumulate at the interface between penatcene and the dielectric and transport along the interface due to the horizontal field effect, followed by injection into the EML beneath the drain electrode and subsequent formation of excitons with the electrons injected from the drain electrode. The electrical activation ordinarily generates 25% singlet excitons and 75% triplet excitons in the EML as is shown in Figure 2b. The singlet excitons can radiate directly from S_1 to S_0, resulting in the prompt fluorescence, while the utilization of triplet excitons from the RISC process results in delayed fluorescence. The efficient RISC process for TCTA/B3PYMPM[37] will facilitate the delayed fluorescence. We can estimate the exciton utilization efficiency by the following equation:[42]

$$\mathrm{EQE} = \gamma \Phi_{\mathrm{spin}} \Phi_{\mathrm{PL}} \Phi_{\mathrm{out}} \quad (1)$$

where γ is the capture efficiency (CE) of electrons and holes injected into the emission layer, Φ_{spin} is the exciton utilization efficiency, Φ_{PL} is the PLQY (36%)[37] of the emitter, and Φ_{out} is the outcoupling efficiency which is assumed to be 0.2−0.3 without any light outcoupling enhancement. Since the capture efficiency can be derived from the following equation considering the exciplex with thermally activated delayed fluorescence,[43]

$$\mathrm{EQE} = \gamma \left[0.25\Phi_{\mathrm{PL}} + 0.75 \frac{\Phi_{\mathrm{DF}}}{1 - (\Phi_{\mathrm{PL}} - \Phi_{\mathrm{DF}})} \right] \Phi_{\mathrm{out}} \quad (2)$$

where Φ_{DF} is the delayed fluorescence efficiency (13%),[37] we can obtain a Φ_{spin} of 60.3%, which is much higher than the theoretical value of 25% for traditional fluorescent emitters.

DOI: 10.1021/acsami.6b13405
ACS Appl. Mater. Interfaces 2017, 9, 2711−2719

It is worth noting that the maximum γ for NPB/HAT-CN modified device is 14.3−21.4% while it is only 0.8−1.2% for TCTA/HAT-CN modified one. The more than 1 order of magnitude improvement for the capture efficiency by virtue of NPB confirms the importance of reducing the energy barrier between the hole transport layer and the donor of the exciplex emitter. Nevertheless, there are still energy barriers between the HOMO levels of NPB and pentacne as well as the EML which may further limit the performance of the device.

To diminish these energy barriers, we next developed and investigated a new kind of exciplex emitter adopting m-MTDATA (molecular structure is presented in Figure 3a) as the donor due to its well aligned HOMO level (−5.1 eV) with that of pentacene. OXD-7 is used as the acceptor. The large energy difference between the HOMO/LUMO levels of m-MTDATA and OXD-7 (~1.4 eV in HOMO level offset and ~0.8 eV in LUMO level offset as shown in Figure 3b) is conducive to the charge accumulation and charge transfer between them to form the exciplex excitons.[44,45] The formation of exciplex in the mixed film of m-MTDATA:OXD-7 can be confirmed by the absorption and photoluminescence (PL) spectra. Figure 3c shows the absorption and photoluminescence (PL) spectra of the pristine m-MTDATA and OXD-7 films and the mixed m-MTDATA:OXD-7 (molar ratio of 1:1) film. In contrast to the pristine films, the absorption spectrum of the mixed film does not show any additional features, indicating weak electronic interactions on the ground state of the mixed film.[46] Meanwhile, the PL spectrum of the mixed film exhibits broadening and obvious red-shift relative to those of the pure m-MTDATA and OXD-7 films. The emission peak of the mixed film centers at 545 nm which corresponds to a photon energy of 2.3 eV which matches well with the energy gap between the HOMO level of m-MTDATA and the LUMO level of OXD-7. These features clearly suggest the formation of exciplex in the mixed film of m-MTDATA:OXD-7.

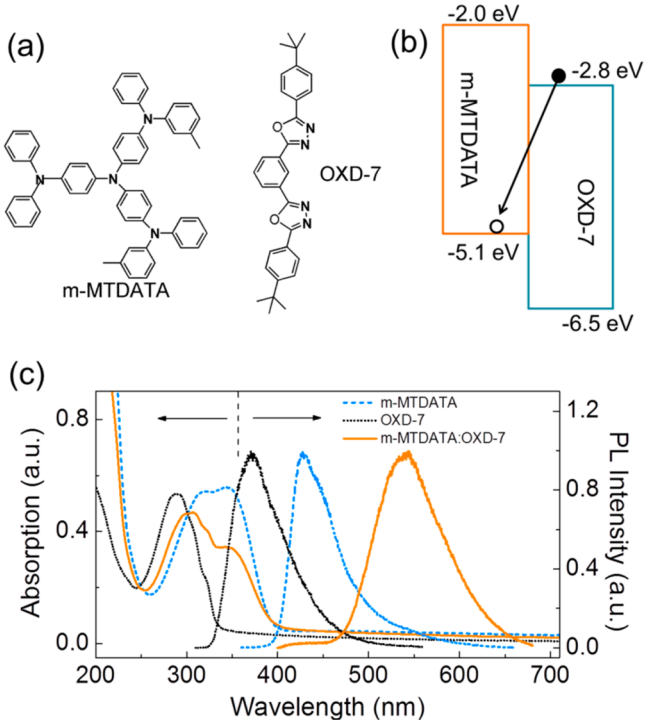

Figure 3. (a) Molecular structures of the donor (m-MTDATA) and acceptor (OXD-7). (b) Schematic diagram of energy levels of m-MTDATA and OXD-7 and exciplex emission formed between them. (c) Absorption and photoluminescence spectra of the pristine m-MTDATA and OXD-7 films and the mixed m-MTDATA:OXD-7 (molar ratio of 1:1) film.

The transient PL decay curves for the mixed film of m-MTDATA:OXD-7 and the pure constituting films at 300 K are shown in Figure 4a and Figure S3, respectively. Both the pure m-MTDATA and OXD-7 films show a single exponential decay with the lifetime of 2.4 and 2.2 ns, respectively. Remarkably, the mixed film exhibits much slower decay which includes a prompt lifetime of 444 ns and a delayed lifetime of 4.96 μs fitted by the double exponential decay function: $I(t) = A_1 \exp(-t/\tau_1) + A_2 \exp(-t/\tau_2)$. Figure 4b shows the time-resolved spectra of the mixed film. The PL spectrum of the prompt component almost overlaps with that of the delayed component, indicating the same transition from S_1 to S_0 (the ground state) for both components and hence demonstrating an up-conversion of the triplet to the singlet excited states via RISC process assisted by the environmental thermal energy. The peak of the PL spectrum for the delayed component represents a slight red-shift in comparison with that of the prompt component, which agrees well with that for other exciplex TADF emitters in the literature[26,31,47] and can probably be ascribed to the broad distribution of the energy levels of the exciplex resulting from the different geometric arrangement between donor and acceptor or the influence of T_1 on the nuclear configuration of the S_1 originated from RISC process.[14,35] The PLQY of the

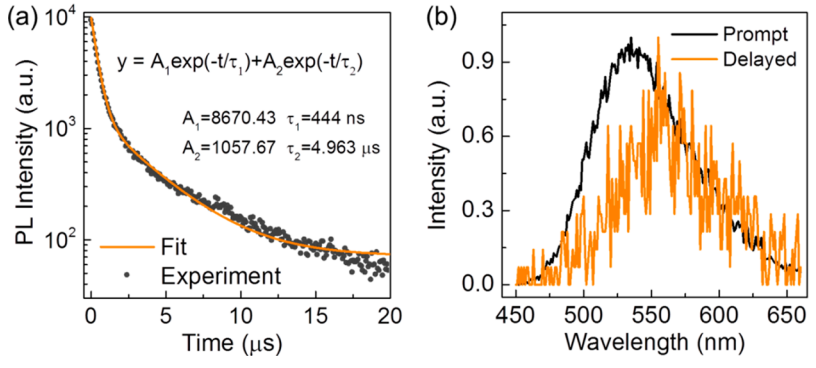

Figure 4. (a) Transient PL decay curves for the mixed film of m-MTDATA:OXD-7 at 300 K monitored at 545 nm. (b) Time-resolved PL spectra of the mixed film at 300 K.

DOI: 10.1021/acsami.6b13405
ACS Appl. Mater. Interfaces 2017, 9, 2711−2719

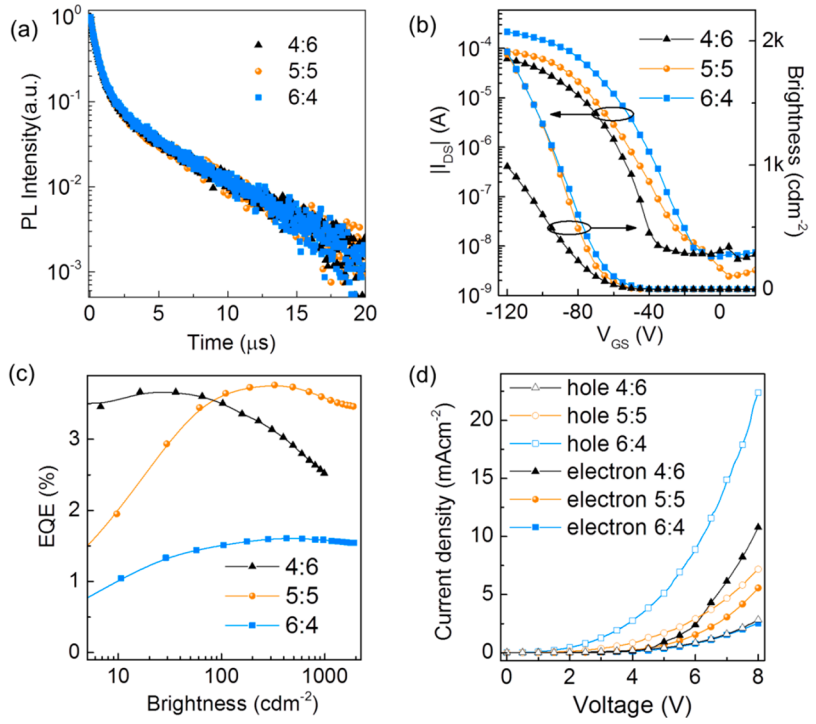

Figure 5. (a) Transient PL decay curves for mixed m-MTDATA:OXD-7 films with different molar ratios. (b) Electrical and optical transfer characteristics and (c) relationship between EQE and brightness for devices with different molar ratios at V_{DS} = −60 V. (d) Current density−voltage curves for hole- and electron-only devices with different molar ratios. Hole-only devices: ITO/exciplex emitter (80 nm)/HAT-CN (5 nm)/Al (100 nm). Electron-only devices: Al (100 nm)/Cs_2CO_3 (3 nm)/exciplex emitter (80 nm)/Cs_2CO_3 (2 nm)/Al (100 nm).

Table 1. Key Electrical and Optical Performance for HOLEFETs with Different Exciplex TADF Emitters

emitter	TCTA:B3PYMPM	m-MTDAT:OXD-7		
molar ratio	1:1	4:6	5:5	6:4
PLQY	36%	28%	28%	25%
hole mobility ($cm^2\ V^{-1}\ s^{-1}$)	0.26	0.04	0.11	0.19
max EQE (%)	0.93	3.66	3.76	1.60
max CE (%)	14.3− 21.4	58.6−87.9	60.2−90.3	29.1−43.7
max brightness (cdm^{-2})	1116	990	1890	1910
on/off ratio	10^4	10^4	10^4	10^4
Φ_{spin}	60.3%	74.3%	74.3%	74.3%

m-MTDATA:OXD-7 film measured using a calibrated integrating sphere is 28% with the prompt fluorescence efficiency (Φ_{PF}) of 11.8% and the delayed fluorescence efficiency (Φ_{DF}) of 16.2%. The efficiency ratio of Φ_{DF}/Φ_{PF} (1.37) is 2.4 times higher than that for TCTA:B3PYMPM (0.56), indicating a more efficient TADF process.[26,37]

Interestingly, the molar ratio between m-MTDATA and OXD-7 makes little influence on the transient PL decay characteristics of the mixed film (see Figure 5a), which means that the delayed component remains unchanged as the molar ratio increases from 4:6 to 5:5 and 6:4. Meanwhile, there are also slight differences in the PLQYs for films with the three molar ratios, which are 28%, 28%, and 25%, respectively.

We subsequently implement the film of m-MTDATA:OXD-7 with different molar ratios as the emission layer in HOLEFETs. Accordingly, m-MTDATA/HAT-CN was used as the OHJ modification layer. The electrical and optical transfer curves for the devices are shown in Figure 5b. All the devices exhibit p-type transport characteristics. As the molar ratio increases from 4:6 to 5:5 and 6:4, the maximum drain current (hole current) increases continuously. This can be attributed to the decreased hole-blocking effect as the proportion of OXD-7 reduces. The hole mobilities extracted from the saturation regions for three devices are 0.04, 0.11, and 0.19 $cm^2\ V^{-1}\ s^{-1}$, respectively (see Table 1). The variation of the hole current for different devices implies that the carrier balance can be tuned by adjusting the molar ratio between m-MTDATA and OXD-7. The brightness for all the devices increases continuously as their respective drain current increases concurrent with a progressively broadened emission zone underneath the drain electrode, indicating that more holes have entered into the EML and formed excitons with the electrons injected from the drain electrode. Figure S4 gives a typical result of the emission zone for device with the molar ratio of 5:5 biased at V_{DS} = −60 V and different V_{GS}. The maximum brightness for devices with the three molar ratios reaches approximately 990, 1890, and 1910 cdm^{-2}, respectively. The characteristics of gate-voltage-dependent light-emission intensity and emission zone width are quite similar to those for

DOI: 10.1021/acsami.6b13405
ACS Appl. Mater. Interfaces 2017, 9, 2711−2719

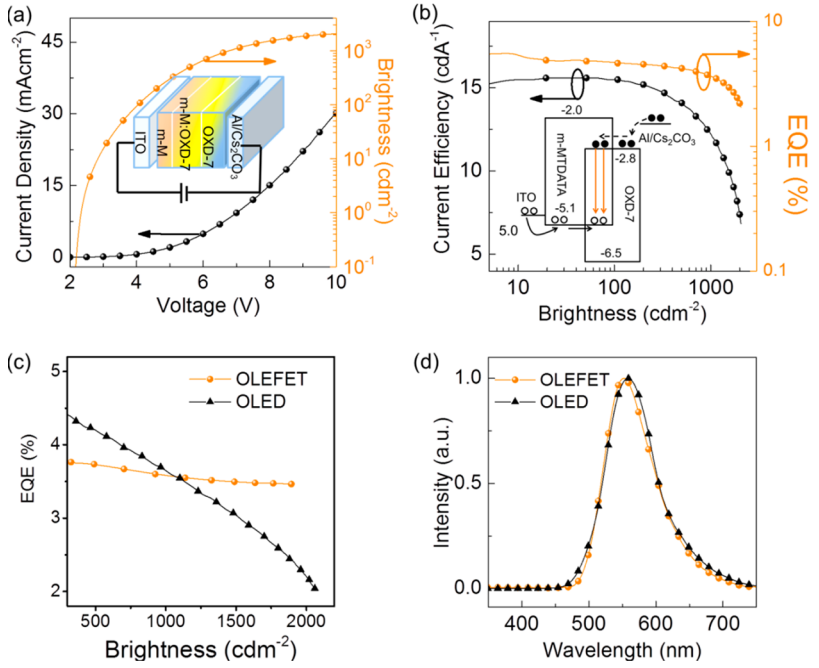

Figure 6. (a) Current density−voltage−brightness curves of OLEDs based on the exciplex emitter of m-MTDATA/OXD-7 (5:5 molar ratio). Inset is the device architecture where m-M stands for m-MTDATA. (b) Current efficiency−brightness−EQE curves of the OLEDs. Inset is the energy schematic diagram for the device. (c) Comparison of EQE between HOLEFET and OLED for different brightness. (d) EL spectra for HOLEFET and OLED.

unipolar HOLEFETs with phosphorescent and fluorescent emitters in the literature.[12,48]

The relationships between the brightness and EQE corresponding to the transfer curves are shown in Figure 5c. The EQE for all the devices shows similar trend including a gradual rising section at low brightness and a slight decrease as the brightness becomes higher. This is the phenomenon of efficiency roll-off as has been widely reported in OLEDs, which can be further interpreted by the corresponding relationships of the drain current versus EQE (Figure S5). The maximum EQE for devices with the molar ratios of 4:6, 5:5 and 6:4 are 3.66% (at 36 cdm^{-2}), 3.76% (at 326 cdm^{-2}), and 1.6% (at 601 cdm^{-2}), respectively. The device with molar ratio of 5:5 shows better performance for the maximum EQE and also exhibits higher value of EQE under high brightness (>100 cdm^{-2}). This can be mainly ascribed to the better balanced carrier transport which can be verified by the current density−voltage curves of the hole-only and electron-only devices with different molar ratios as shown in Figure 5d. As the proportion of m-MTDATA increases, the hole current density increases while the electron current density decreases. The hole current and electron currents become more balanced for the molar ratio of 5:5 than the others. The maximum γ calculated by eq 2 for the device with molar ratio of 5:5 (60.2−90.3%) is also much higher than the results for devices with molar ratio of 4:6 (58.6−87.9%) and 6:4 (29.1−43.7%). These results reveal the importance of optimizing the molar ratio of the donor and acceptor for HOLEFETs with exciplex emitters. It is worth noting that the maximum γ is more than 4 times higher for devices with exciplex TADF emitter of m-MTDATA:OXD-7 than TCTA:B3PYMPM, which also confirms the significance of reducing the energy barrier between the hole transport layer and exciplex emission layer. The resulting Φ_{spin} from eq 1 reaches as high as 74.3%, demonstrating better utilization of the triplet excitons than that for devices with exciplex TADF emitter of TCTA:B3PYMPM.

OLEDs using m-MTDATA:OXD-7 (molar ratio 5:5) as the EML (inset of Figure 6a) were also fabricated for a further comparison. Optimized optoelectrical properties for the device are presented in Figure 6a and Figure 6b. The turn-on voltage is only 2.35 V which is close to the photon energy of the emitted light divided by the elementary charge. The low turn-on voltage suggests that there is small energy barrier for the hole and electron injection into the EML as shown in the inset of Figure 6b. The device shows moderate values of 2060 cdm^{-2}, 5.6%, and 15.6 c dA^{-1} for the maximum brightness, EQE, and current efficiency, respectively. Figure 6c compares the EQE for HOLEFETs and OLEDs at different brightness. It is noticed that the HOLEFET shows much smaller efficiency roll-off. The EQE of HOLEFETs keeps at about 3.5% and outperforms that of the OLEDs when the brightness is higher than 1100 cdm^{-2}. The smaller efficiency roll-off for HOLEFETs can be ascribed to the separated regions for charge transport and exciton formation, which can suppress the exciton−charge interactions.[10] To the best of our knowledge, this is the first time that the emission characteristic of a HOLEFET can truly compare with that of an OLED using the same emitter at high brightness.[13,15−17,22,49−51] The EL spectra for both the HOLEFETs and OLEDs are shown in Figure 6d with peak wavelength at 555 nm, which resemble the PL spectrum, indicating good restriction of excitons in the EML.

The high EQE for the HOLEFETs with exciplex TADF emitter of m-MTDATA:OXD-7 mainly benefits from the efficient utilization of triplet excitons and well-matched HOMO levels due to the judiciously selected exciplex materials. However, the exciplex of m-MTDATA:OXD-7 still suffers from the drawback of low PLQY. Besides, despite the relatively high capture efficiency achieved in the unipolar HOLEFETs, the lack of electron transport layer with high mobility restrains

DOI: 10.1021/acsami.6b13405
ACS Appl. Mater. Interfaces 2017, 9, 2711−2719

the emission zone mainly beneath the drain electrode where a large amount of electrons injected and accumulated, which may also lead to the exciton-charge quenching loss.[10] Therefore, strategies such as doping the exciplex with efficient fluorescent materials[52] or exploring novel exciplex TADF materials to improve the PLQY[47] and introducing electron transport layer with high mobility or implementing nonplanar asymmetrical S/D electrodes[18] to promote the electron injection and transport can be considered to further soar the performance of such devices.

CONCLUSION

In summary, HOLEFETs implementing different exciplex TADF emitters have been investigated. By virtue of harvesting the triplet excitons, the device with the exciplex of TCTA:B3PYMPM showed a maximum EQE of 0.93%, which is comparable to the state-of-the-art results for devices with conventional fluorescent emitters despite the large hole injection barrier. The implementation of a new exciplex TADF emitter of m-MTDATA:OXD-7 further reduced the hole injection barrier and improved the exciton utilization efficiency to as high as 74.3%. Together with a careful adjustment of the carrier balance by changing the mole ratios of m-MTDATA and OXD-7, devices with excellent performance of a maximum EQE of 3.76% and an on/off ratio of $\sim 10^4$ were demonstrated. Moreover, the EQE at high brightness even outperforms the result for OLED based on the same emitter. The results not only demonstrate that the exciplex TADF emitters can be promising candidates for developing colorful and low-cost HOLEFETs with high performance but also open a way to explore the full potential of the emission layer for HOLEFETs.

EXPERIMENTAL SECTION

Film Fabrication and Characterization. The pure m-MTDATA (50 nm), OXD-7 (50 nm), TCTA (40 nm), HAT-CN (40 nm) films, mixed film of m-MTDATA:OXD-7 (50 nm with molar ratio 1:1) and HAT-CN-doped TCTA film (40 nm, 50 mol % HAT-CN) were thermally evaporated onto the quartz glass to measure their optical characteristics.

The UV−vis−NIR absorption spectra of these films were performed with a Shimadzu UV-3101PC UV−vis−NIR spectrophotometer. PL spectra were measured using Hitachi florescence spectrometer F-7000. Absolute fluorescent quantum yield measurements, transient PL decay properties, and time-resolved spectra were performed by Edinburgh FLS920 spectrometer.

Device Fabrication and Characterization. The poly(4-vinylphenol) (PVP, 420 nm) was spin-coated onto indium tin oxide (ITO) glass substrates using solution prepared with PVP and poly(melamine-*co*-formaldehyde) (2:1 wt %) in propylene glycol monomethyl ether acetate (PGMEA) (90 mg/mL) and then annealed at 200 °C for 1 h.The polystyrene (PS, 30 nm) dissolved in toluene (6 mg/mL) was successively spin-coated (30 s at 3000 rpm) on PVP and annealed at 85 °C for 1 h. Pentacene (14 nm), hole injection layer (10 nm, TCTA or NPB or m-MTDATA), HAT-CN (1 nm), emission layer (30 nm, TCTA:B3PYMPM or m-MTDATA:OXD-7), electron injection layer (20 nm, Bphen or OXD-7), Cs_2CO3 (1 nm), and Al (1 nm), were successively thermal evaporated with the rate of 0.2, 0.3, 0.1, 2, 0.3 0.2, and 0.2 Å/s, respectively. Ag was thermally deposited through a shadow mask with channel length and width of 45 and 3000 μm, respectively. For the fabrication of OLED, m-MTDATA (30 nm), m-MTDATA:OXD-7 (45 nm), OXD-7 (35 nm), Cs_2CO_3 (1 nm) were subsequently thermally deposited onto the ITO glass substrates with the rate of 2, 4, 2, 0.5 Å/s, respectively. The Al electrode (40 nm) was then thermally deposited with the rate of 4 Å/s. All the devices were encapsulated with UV glue in the glovebox (H_2O, O_2 < 0.1 ppm) before testing. The light emission was detected from the ITO side.

The brightness and current density of OLEDs were measured using a Keithley 2400 source meter and a luminance meter KONICA MINOLTA LS-110. The electrical characteristics of HOLEFETs were performed by Keithley 4200 SCS at room temperature under air ambient. The photocurrent was recorded by HAMAMATSU S1336 photodiode. The optical images were captured by Olympus BX51TRF CCD microscope. The electroluminescence spectra were measured by AvaSpec-ULS2048L fiber spectrometer. The brightness for HOLEFETs was calculated by comparing the photocurrent with the fabricated OLED at fixed brightness (500 cdm^{-2}) and emission area (2 mm × 3 mm). The EQE for HOLEFETs was calculated from the brightness, the drain current, and the EL emission spectrum assuming Lambertian emission. The carrier mobilities were calculated by the formula for the saturation regime: $I_{DS} = \mu C_i[W/(2L)](V_{GS} - V_T)^2$ (where μ is the field-effect mobility, C_i is the gate dielectric capacitance density, V_T is the threshold voltage, and W and L are the channel width and length, respectively).

ASSOCIATED CONTENT

Supporting Information

The Supporting Information is available free of charge on the ACS Publications website at DOI: 10.1021/acsami.6b13405.

UV−vis−NIR absorption spectra and transfer for OLEFETs without OHJ (Figure S1), molecular structures (Figure S2), transient PL decay properties for m-MTDATA, OXD-7 (Figure S3), microphotographs for HOLEFET and the determination of the emission zone width (Figure S4), and EQE versus drain current (Figure S5) (PDF)

AUTHOR INFORMATION

Corresponding Authors

*Y.H.: e-mail, huyongsheng@ciomp.ac.cn.
*X.L.: e-mail, liuxy@ciomp.ac.cn.

ORCID

Yongsheng Hu: 0000-0002-8116-4378
Ying Lv: 0000-0003-1649-5258
Xiaoyang Guo: 0000-0003-0259-137X
Xingyuan Liu: 0000-0002-9681-1646

Notes

The authors declare no competing financial interest.

ACKNOWLEDGMENTS

This work was funded by National Natural Science Foundation of China Grants 6140031454 and 51503196 and Jilin Province Science and Technology Research Projects 20160520092JH and 20160520176JH.

REFERENCES

(1) Bisri, S. Z.; Piliego, C.; Gao, J.; Loi, M. A. Outlook and Emerging Semiconducting Materials for Ambipolar Transistors. *Adv. Mater.* **2014**, *26*, 1176−1199.

(2) Hotta, S.; Yamao, T.; Bisri, S. Z.; Takenobu, T.; Iwasa, Y. Organic Single-Crystal Light-Emitting Field-Effect Transistors. *J. Mater. Chem. C* **2014**, *2*, 965−980.

(3) Muccini, M.; Koopman, W.; Toffanin, S. The Photonic Perspective of Organic Light-Emitting Transistors. *Laser Photonics Rev.* **2012**, *6*, 258−275.

(4) Takenobu, T.; Bisri, S. Z.; Takahashi, T.; Yahiro, M.; Adachi, C.; Iwasa, Y. High Current Density in Light-Emitting Transistors of Organic Single Crystals. *Phys. Rev. Lett.* **2008**, *100*, 066601.

DOI: 10.1021/acsami.6b13405
ACS Appl. Mater. Interfaces 2017, 9, 2711−2719

(5) Cicoira, F.; Santato, C. Organic Light Emitting Field Effect Transistors: Advances and Perspectives. *Adv. Funct. Mater.* **2007**, *17*, 3421−3434.
(6) Zaumseil, J.; Sirringhaus, H. Electron and Ambipolar Transport in Organic Field-Effect Transistors. *Chem. Rev.* **2007**, *107*, 1296−1323.
(7) Gwinner, M. C.; Kabra, D.; Roberts, M.; Brenner, T. J. K.; Wallikewitz, B. H.; McNeill, C. R.; Friend, R. H.; Sirringhaus, H. Highly Efficient Single-Layer Polymer Ambipolar Light-Emitting Field-Effect Transistors. *Adv. Mater.* **2012**, *24*, 2728−2734.
(8) Yamao, T.; Sakurai, Y.; Terasaki, K.; Shimizu, Y.; Jinnai, H.; Hotta, S. Current-Injected Spectrally-Narrowed Emissions from an Organic Transistor. *Adv. Mater.* **2010**, *22*, 3708−3712.
(9) Capelli, R.; Dinelli, F.; Loi, M. A.; Murgia, M.; Zamboni, R.; Muccini, M. Ambipolar Organic Light-Emitting Transistors Employing Heterojunctions of N-Type and P-Type Materials as the Active Layer. *J. Phys.: Condens. Matter* **2006**, *18*, S2127−S2138.
(10) Capelli, R.; Toffanin, S.; Generali, G.; Usta, H.; Facchetti, A.; Muccini, M. Organic Light-Emitting Transistors with an Efficiency That Outperforms the Equivalent Light-Emitting Diodes. *Nat. Mater.* **2010**, *9*, 496−503.
(11) Ullah, M.; Tandy, K.; Yambem, S. D.; Aljada, M.; Burn, P. L.; Meredith, P.; Namdas, E. B. Simultaneous Enhancement of Brightness, Efficiency, and Switching in RGB Organic Light Emitting Transistors. *Adv. Mater.* **2013**, *25*, 6213−6218.
(12) Ullah, M.; Wawrzinek, R.; Maasoumi, F.; Lo, S.-C.; Namdas, E. B. Semitransparent and Low-Voltage Operating Organic Light-Emitting Field-Effect Transistors Processed at Low Temperatures. *Adv. Opt. Mater.* **2016**, *4*, 1022−1026.
(13) Song, L.; Hu, Y. S.; Zhang, N.; Li, Y. T.; Lin, J.; Liu, X. Y. Improved Performance of Organic Light-Emitting Field-Effect Transistors by Interfacial Modification of Hole-Transport Layer/Emission Layer: Incorporating Organic Heterojunctions. *ACS Appl. Mater. Interfaces* **2016**, *8*, 14063−14070.
(14) Ullah, M.; Tandy, K.; Li, J.; Shi, Z.; Burn, P. L.; Meredith, P.; Namdas, E. B. High-Mobility, Heterostructure Light-Emitting Transistors and Complementary Inverters. *ACS Photonics* **2014**, *1*, 954−959.
(15) Ullah, M.; Tandy, K.; Yambem, S. D.; Muhieddine, K.; Ong, W. J.; Shi, Z.; Burn, P. L.; Meredith, P.; Li, J.; Namdas, E. B. Efficient and Bright Polymer Light Emitting Field Effect Transistors. *Org. Electron.* **2015**, *17*, 371−376.
(16) Yambem, S. D.; Ullah, M.; Tandy, K.; Burn, P. L.; Namdas, E. B. ITO-Free Top Emitting Organic Light Emitting Diodes with Enhanced Light out-Coupling. *Laser Photonics Rev.* **2014**, *8*, 165−171.
(17) Tanaka, D.; Sasabe, H.; Li, Y. J.; Su, S. J.; Takeda, T.; Kido, J. Ultra High Efficiency Green Organic Light-Emitting Devices. *Jpn. J. Appl. Phys., Part 2* **2007**, *46*, L10−L12.
(18) Muhieddine, K.; Ullah, M.; Maasoumi, F.; Burn, P. L.; Namdas, E. B. Hybrid Area-Emitting Transistors: Solution Processable and with High Aperture Ratios. *Adv. Mater.* **2015**, *27*, 6677−6682.
(19) Seo, J. H.; Namdas, E. B.; Gutacker, A.; Heeger, A. J.; Bazan, G. C. Conjugated Polyelectrolytes for Organic Light Emitting Transistors. *Appl. Phys. Lett.* **2010**, *97*, 043303.
(20) Lee, D. R.; Kim, B. S.; Lee, C. W.; Im, Y.; Yook, K. S.; Hwang, S.-H.; Lee, J. Y. Above 30% External Quantum Efficiency in Green Delayed Fluorescent Organic Light-Emitting Diodes. *ACS Appl. Mater. Interfaces* **2015**, *7*, 9625−9629.
(21) Baldo, M. A.; O'Brien, D. F.; You, Y.; Shoustikov, A.; Sibley, S.; Thompson, M. E.; Forrest, S. R. Highly Efficient Phosphorescent Emission from Organic Electroluminescent Devices. *Nature* **1998**, *395*, 151−154.
(22) Namdas, E. B.; Hsu, B. B. Y.; Liu, Z.; Lo, S.-C.; Burn, P. L.; Samuel, I. D. W. Phosphorescent Light-Emitting Transistors: Harvesting Triplet Excitons. *Adv. Mater.* **2009**, *21*, 4957−4961.
(23) Wang, Y.; Lu, Y.; Gao, B.; Wang, S.; Ding, J.; Wang, L.; Jing, X.; Wang, F. Self-Host Blue-Emitting Iridium Dendrimer Containing Bipolar Dendrons for Nondoped Electrophosphorescent Devices with Superior High-Brightness Performance. *ACS Appl. Mater. Interfaces* **2016**, *8*, 29600−29607.
(24) Kawamura, Y.; Goushi, K.; Brooks, J.; Brown, J. J.; Sasabe, H.; Adachi, C. 100% Phosphorescence Quantum Efficiency of Ir(III) Complexes in Organic Semiconductor Films. *Appl. Phys. Lett.* **2005**, *86*, 071104.
(25) Endo, A.; Sato, K.; Yoshimura, K.; Kai, T.; Kawada, A.; Miyazaki, H.; Adachi, C. Efficient up-Conversion of Triplet Excitons into a Singlet State and Its Application for Organic Light Emitting Diodes. *Appl. Phys. Lett.* **2011**, *98*, 083302.
(26) Goushi, K.; Yoshida, K.; Sato, K.; Adachi, C. Organic Light-Emitting Diodes Employing Efficient Reverse Intersystem Crossing for Triplet-to-Singlet State Conversion. *Nat. Photonics* **2012**, *6*, 253−258.
(27) Tao, Y.; Yuan, K.; Chen, T.; Xu, P.; Li, H.; Chen, R.; Zheng, C.; Zhang, L.; Huang, W. Thermally Activated Delayed Fluorescence Materials Towards the Breakthrough of Organoelectronics. *Adv. Mater.* **2014**, *26*, 7931−7958.
(28) Li, C.; Duan, L.; Zhang, D.; Qiu, Y. Thermally Activated Delayed Fluorescence Sensitized Phosphorescence: A Strategy to Break the Trade-Off between Efficiency and Efficiency Roll-Off. *ACS Appl. Mater. Interfaces* **2015**, *7*, 15154−15159.
(29) Uoyama, H.; Goushi, K.; Shizu, K.; Nomura, H.; Adachi, C. Highly Efficient Organic Light-Emitting Diodes from Delayed Fluorescence. *Nature* **2012**, *492*, 234−238.
(30) Goushi, K.; Adachi, C. Efficient Organic Light-Emitting Diodes through up-Conversion from Triplet to Singlet Excited States of Exciplexes. *Appl. Phys. Lett.* **2012**, *101*, 023306.
(31) Hung, W.-Y.; Fang, G.-C.; Chang, Y.-C.; Kuo, T.-Y.; Chou, P.-T.; Lin, S.-W.; Wong, K.-T. Highly Efficient Bilayer Interface Exciplex for Yellow Organic Light-Emitting Diode. *ACS Appl. Mater. Interfaces* **2013**, *5*, 6826−6831.
(32) Hung, W.-Y.; Fang, G.-C.; Lin, S.-W.; Cheng, S.-H.; Wong, K.-T. p.; Kuo, T.-Y.; Chou, P.-T. The First Tandem, All-Exciplex-Based WOLED. *Sci. Rep.* **2014**, *4*, 5161.
(33) Zhao, B.; Zhang, T.; Chu, B.; Li, W.; Su, Z.; Wu, H.; Yan, X.; Jin, F.; Gao, Y.; Liu, C. Highly Efficient Red OLEDs Using DCJTB as the Dopant and Delayed Fluorescent Exciplex as the Host. *Sci. Rep.* **2015**, *5*, 10697.
(34) Seino, Y.; Sasabe, H.; Pu, Y.-J.; Kido, J. High-Performance Blue Phosphorescent Oleds Using Energy Transfer from Exciplex. *Adv. Mater.* **2014**, *26*, 1612−1616.
(35) Su, S.-J.; Cai, C.; Takamatsu, J.; Kido, J. A Host Material with a Small Singlet-Triplet Exchange Energy for Phosphorescent Organic Light-Emitting Diodes: Guest, Host, and Exciplex Emission. *Org. Electron.* **2012**, *13*, 1937−1947.
(36) Wang, S.; Wang, X.; Yao, B.; Zhang, B.; Ding, J.; Xie, Z.; Wang, L. Solution-Processed Phosphorescent Organic Light-Emitting Diodes with Ultralow Driving Voltage and Very High Power Efficiency. *Sci. Rep.* **2015**, *5*, 12487.
(37) Park, Y.-S.; Kim, K.-H.; Kim, J.-J. Efficient Triplet Harvesting by Fluorescent Molecules through Exciplexes for High Efficiency Organic Light-Emitting Diodes. *Appl. Phys. Lett.* **2013**, *102*, 153306.
(38) Nakanotani, H.; Kabe, R.; Yahiro, M.; Takenobu, T.; Iwasa, Y.; Adachi, C. Blue-Light-Emitting Ambipolar Field-Effect Transistors Using an Organic Single Crystal of 1,4-Bis(4-Methylstyryl)Benzene. *Appl. Phys. Express* **2008**, *1*, 091801.
(39) Kajii, H.; Tanaka, H.; Kusumoto, Y.; Ohtomo, T.; Ohmori, Y. In-Plane Light Emission of Organic Light-Emitting Transistors with Bilayer Structure Using Ambipolar Semiconducting Polymers. *Org. Electron.* **2015**, *16*, 26−33.
(40) Ullah, M.; Armin, A.; Tandy, K.; Yambem, S. D.; Burn, P. L.; Meredith, P.; Namdas, E. B. Defining the Light Emitting Area for Displays in the Unipolar Regime of Highly Efficient Light Emitting Transistors. *Sci. Rep.* **2015**, *5*, 8818.
(41) Sun, H.; Guo, Q.; Yang, D.; Chen, Y.; Chen, J.; Ma, D. High Efficiency Tandem Organic Light Emitting Diode Using an Organic Heterojunction as the Charge Generation Layer: An Investigation into the Charge Generation Model and Device Performance. *ACS Photonics* **2015**, *2*, 271−279.
(42) Ouyang, X.; Li, X.-L.; Ai, L.; Mi, D.; Ge, Z.; Su, S.-J. Novel "Hot Exciton" Blue Fluorophores for High Performance Fluorescent/

DOI: 10.1021/acsami.6b13405
ACS Appl. Mater. Interfaces 2017, 9, 2711−2719

Phosphorescent Hybrid White Organic Light-Emitting Diodes with Superhigh Phosphorescent Dopant Concentration and Improved Efficiency Roll-Off. *ACS Appl. Mater. Interfaces* **2015**, *7*, 7869−7877.
(43) Wang, Z.; Li, Y.; Cai, X.; Chen, D.; Xie, G.; Liu, K.; Wu, Y.-C.; Lo, C.-C.; Lien, A.; Cao, Y.; Su, S.-J. Structure-Performance Investigation of Thioxanthone Derivatives for Developing Color Tunable Highly Efficient Thermally Activated Delayed Fluorescence Emitters. *ACS Appl. Mater. Interfaces* **2016**, *8*, 8627−8636.
(44) Hung, W.-Y.; Chiang, P.-Y.; Lin, S.-W.; Tang, W.-C.; Chen, Y.-T.; Liu, S.-H.; Chou, P.-T.; Hung, Y.-T.; Wong, K.-T. Balance the Carrier Mobility to Achieve High Performance Exciplex OLED Using a Triazine-Based Acceptor. *ACS Appl. Mater. Interfaces* **2016**, *8*, 4811−4818.
(45) Zhang, T.; Chu, B.; Li, W.; Su, Z.; Peng, Q. M.; Zhao, B.; Luo, Y.; Jin, F.; Yan, X.; Gao, Y.; Wu, H.; Zhang, F.; Fan, D.; Wang, J. Efficient Triplet Application in Exciplex Delayed-Fluorescence OLEDs Using a Reverse Intersystem Crossing Mechanism Based on a Delta Es-T of around Zero. *ACS Appl. Mater. Interfaces* **2014**, *6*, 11907−11914.
(46) Chen, D.; Wang, Z.; Wang, D.; Wu, Y.-C.; Lo, C.-C.; Lien, A.; Cao, Y.; Su, S.-J. Efficient Exciplex Organic Light-Emitting Diodes with a Bipolar Acceptor. *Org. Electron.* **2015**, *25*, 79−84.
(47) Li, J.; Nomura, H.; Miyazaki, H.; Adachi, C. Highly Efficient Exciplex Organic Light-Emitting Diodes Incorporating a Heptazine Derivative as an Electron Acceptor. *Chem. Commun.* **2014**, *50*, 6174−6176.
(48) Ullah, M.; Lin, Y.-H.; Muhieddine, K.; Lo, S.-C.; Anthopoulos, T. D.; Namdas, E. B. Hybrid Light-Emitting Transistors Based on Low-Temperature Solution-Processed Metal Oxides and a Charge-Injecting Interlayer. *Adv. Opt. Mater.* **2016**, *4*, 231−237.
(49) Toffanin, S.; Capelli, R.; Koopman, W.; Generali, G.; Cavallini, S.; Stefani, A.; Saguatti, D.; Ruani, G.; Muccini, M. Organic Light-Emitting Transistors with Voltage-Tunable Lit Area and Full Channel Illumination. *Laser Photonics Rev.* **2013**, *7*, 1011−1019.
(50) Baldo, M. A.; O'Brien, D. F.; Thompson, M. E.; Forrest, S. R. Excitonic Singlet-Triplet Ratio in a Semiconducting Organic Thin Film. *Phys. Rev. B: Condens. Matter Mater. Phys.* **1999**, *60*, 14422−14428.
(51) Ribierre, J. C.; Stevenson, S. G.; Samuel, I. D. W.; Staton, S. V.; Burn, P. L. Optimization of the Luminescence Efficiencies in Solution-Processed Phosphorescent Dendrimers. *J. Disp. Technol.* **2007**, *3*, 233−237.
(52) Zhou, D.-Y.; Siboni, H. Z.; Wang, Q.; Liao, L.-S.; Aziz, H. Host to Guest Energy Transfer Mechanism in Phosphorescent and Fluorescent Organic Light-Emitting Devices Utilizing Exciplex-Forming Hosts. *J. Phys. Chem. C* **2014**, *118*, 24006−24012.

DOI: 10.1021/acsami.6b13405
ACS Appl. Mater. Interfaces 2017, 9, 2711−2719